Scattering from a Periodic Array on a Semi-infinite Dielectric Substrate

Scattering from a Periodic Array on a Semi-infinite Dielectric Substrate

Hideaki WAKABAYASHI*, Masanobu KOMINAMI*
and Shinnosuke SAWA*

Frequency Selective Screen (*FSS*) is used for a device to execute synchronous reception of multi-frequency. The *FSS* is often used over the dielectric lens. In this paper, the *FSS* over the large dielectric lens is considered and the scattering problem by an arbitrary shaped periodic array on a semi-infinite dielectric substrate is analyzed. The equivalent electric and magnetic currents evaluated by the boundary conditions are introduced. In addition, the current induced on conductor is expanded in a Fourier series corresponding to Floquet modes and this current distribution is determined by the moment method in the spectral domain. Numerical results are given and this theory is verified in comparison with the results of other papers.

1. Introduction

The problem of scattering from Frequency Selective Screen (*FSS*) consisting of an infinite periodic array in free space or on a relatively thin dielectric substrate is reported in many papers. For the effective use of frequencies in satellite communication and the radio astronomical observation, the *FSS* which executes synchronous reception of multi-frequency is important[1]. Particularly, a decision on spectrum of solar flares of which phenomenon changes fast and a investigation for cosmic rays require the identity in time and space. So we can use the *FSS* which executes synchronous reception of multi-frequency.

The *FSS* is a metallic grating printed on the surface of a dielectric substrate. Usually by making the dielectric substrate electrically thin, the effect of surface waves propagating along the substrate is avoided. But at millimeter wave frequencies, the thickness may not be ignored. In addition, the *FSS* is often used over the dielectric lens. Accordingly, in this paper, we will consider the *FSS* over the large dielectric lens and analyze the scattering problem by a periodic array of arbitrarily shaped elements on semi-infinite dielectric substrate.

* Department of Electrical Engineering, College of Engineering

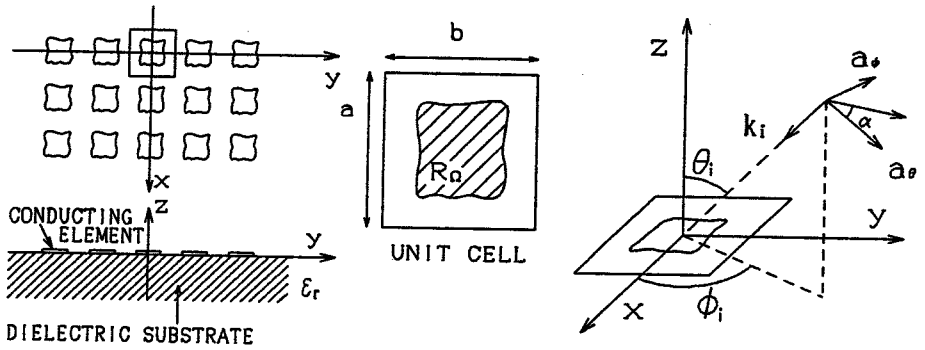

Fig. 1 Geometry of considered scatterer.

2. Theory

2. 1 The incident field and the current distribution

The geometry considered here is shown in Fig.1. An infinite periodic array of arbitrarily shaped conducting elements with periodicities of a and b in the x and y directions is printed on a semi-infinite dielectric substrate which has relative dielectric constant ε_r. The element has resistance R Ω per unit square and is electrically so thin compared with wave-length that the thickness can be neglected. The *FSS* is assumed to be illuminated by an incident plane wave propagating from (θ_i, ϕ_i) direction. The incident field is given by

$$\begin{aligned} \boldsymbol{E}_i(x, y, z) &= \boldsymbol{E}_{io} e^{-j\boldsymbol{k}_i \cdot \boldsymbol{r}} \\ \boldsymbol{H}_i(x, y, z) &= \boldsymbol{H}_{io} e^{-j\boldsymbol{k}_i \cdot \boldsymbol{r}} \\ \boldsymbol{H}_{io} &= \boldsymbol{k}_i \times \boldsymbol{E}_{io} / \omega \mu_o \end{aligned} \tag{1}$$

where $\boldsymbol{r}$ is a position vector and $\boldsymbol{k}_i$ is a propagation vector of the incident plane wave. By using unit vectors $(\boldsymbol{a}_x, \boldsymbol{a}_y, \boldsymbol{a}_z)$ in the (x, y, z) direction, $\boldsymbol{r}$ and $\boldsymbol{k}_i$ can be written as

$$\begin{aligned} \boldsymbol{r} &= x\boldsymbol{a}_x + y\boldsymbol{a}_y + z\boldsymbol{a}_z \\ \boldsymbol{k}_i &= k_{ix}\boldsymbol{a}_x + k_{iy}\boldsymbol{a}_y - \gamma_i \boldsymbol{a}_z \end{aligned} \tag{2}$$

with

$$\begin{aligned} k_{ix} &= -k_i \sin\theta_i \cos\theta_i \\ k_{iy} &= -k_i \sin\theta_i \sin\theta_i \\ \gamma_i &= \sqrt{k_i^2 - k_{ix}^2 - k_{iy}^2}. \end{aligned} \tag{3}$$

In addition, $\boldsymbol{E}_{io}$ is an amplitude vector of the incident electric field and by using the unit vectors:

$$\begin{aligned} \boldsymbol{a}_\theta &= \cos\theta_i \cos\phi_i \, \boldsymbol{a}_x + \cos\theta_i \sin\phi_i \boldsymbol{a}_y - \sin\theta_i \boldsymbol{a}_z \\ \boldsymbol{a}_\phi &= -\sin\phi_i \, \boldsymbol{a}_x + \cos\phi_i \, \boldsymbol{a}_y, \end{aligned} \tag{4}$$

we have

$$\boldsymbol{E}_{io} = \boldsymbol{E}_{i\theta} \, \boldsymbol{a}_\theta + \boldsymbol{E}_{i\phi} \, \boldsymbol{a}_\phi. \tag{5}$$

In the case of linerly-polarized wave, $\boldsymbol{E}_{i\theta}$ and $\boldsymbol{E}_{i\phi}$ are given by

$$\boldsymbol{E}_{i\theta} = \cos\alpha, \quad \boldsymbol{E}_{i\phi} = \sin\alpha$$

where α is a polarized angle on the (θ_i, ϕ_i) plane normal to the wave propagating direction.

We assumed that $\boldsymbol{J}_c$ is an electric current induced on the conductor due to the incident wave $\boldsymbol{E}_i$. Radiation from the current $\boldsymbol{J}_c$ and scattering from the dielectric substrate yield the electromagnetic field.

The current induced on the conductor is proportional to the phase of the incident wave in Eq.(1) and is expanded in a Fourier series corresponding to Floquet modes, since the structure is periodic. The current is given by

$$\boldsymbol{J}_c(x, y) = \sum_{p=-\infty}^{\infty} \sum_{q=-\infty}^{\infty} \boldsymbol{J}_{pq} \, e^{-j(k_{xp}x + k_{yq}y)} \tag{6}$$

where

$$\begin{aligned} k_{xp} &= 2\pi p/a + k_{ix} \\ k_{yq} &= 2\pi q/b + k_{iy}. \end{aligned}$$

In order to evaluate the coefficient $\boldsymbol{J}_{pq}$, both sides of Eq.(6) is multiplied by

$$e^{j(k_{xp}'x + k_{yq}'y)}$$

and then integrated over the unit cell area. The result is

$$\boldsymbol{J}_{pq} = \frac{1}{ab} \widetilde{\boldsymbol{J}}_{co}(k_{xp}, k_{yq}) \tag{7}$$

where $\widetilde{\boldsymbol{J}}_{co}(k_{xp}, k_{yq})$ is Fourier transform of the electric current distribution $\boldsymbol{J}_{co}(x, y)$ on the conducting element. Substituting the Fourier transform Eq.(7) into Eq.(6), we can express the current distribution as

$$\boldsymbol{J}_c = \frac{1}{ab} \sum_{p=-\infty}^{\infty} \sum_{q=-\infty}^{\infty} \widetilde{\boldsymbol{J}}_{co}(k_{xp}, k_{yq}) \, e^{-j(k_{xp}x + k_{yq}y)}. \tag{8}$$

2. 2 The moment method

J_c is the electric current induced on the conductor due to the incident wave (E_i, H_i). (E_1, H_1) and (E_2, H_2) are electromagnetic fields at the air-dielectric interface scattered from the conductor and from the surface of the dielectric substrate. The boundary conditions have to be satisfied as

$$(E_1 + E_i - E_2) \times a_z = 0 \quad \text{(on dielectric substrate)} \tag{9a}$$
$$a_z \times (H_1 + H_i - H_2) = J_c \quad \text{(on conductor)} \tag{9b}$$
$$(E_1 + E_i) \times a_z = RJ_c \quad \text{(on conductor).} \tag{9c}$$

In order to treat the scattered field both from the conductor and from the surface of the dielectric substrate in a unified formulation, we introduce the equivalent electric current J_i and the equivalent magnetic current M_i, given by

$$\begin{aligned} J_i(x, y) &= H_i(x, y, 0) \times a_z \\ M_i(x, y) &= a_z \times E_i(x, y, 0) . \end{aligned} \tag{10}$$

Therefore, we can treat the scattered field from the surface of the dielectric substrate as the radiation from the sources of the equivalent electric and magnetic currents. Then, we can express the scattered field by the Green's function. By using Eq.(1), the equivalent electric and magnetic currents can be written as

$$\begin{aligned} J_i(x, y) &= J_{i0} e^{-jk_i \cdot r} \\ M_i(x, y) &= M_{i0} e^{-jk_i \cdot r} \end{aligned} \tag{11}$$

with

$$\begin{aligned} J_{i0} &= H_{i0} \times a_z \\ M_{i0} &= a_z \times E_{i0}. \end{aligned}$$

Since the structure considered here consists of two homogeneous layers, *i.e.*, the dielectric substrate and air regions, the scattered field is expressed as hybrid-mode. The Green's function can not be written in a closed-form expression but can be treated as integral form in the spectral domain. We now define a Fourier transform pair as

$$\begin{aligned} \tilde{f}(k_x, k_y) &= \iint_{-\infty}^{\infty} f(x, y)\, e^{j(k_x x + k_y y)}\, dxdy \\ f(x, y) &= \frac{1}{4\pi^2} \iint_{-\infty}^{\infty} \tilde{f}(k_x, k_y)\, e^{-j(k_x x + k_y y)}\, dk_x dk_y. \end{aligned} \tag{12}$$

The tilde over a quantity designates the Fourier transform of that quantity. The Fourier transforms of Eqs.(8) and (11) can be written as

$$\tilde{\boldsymbol{J}}_c(k_x, k_y) = \frac{1}{ab}\sum_p\sum_q \tilde{\boldsymbol{J}}_{co}(k_x, k_y)4\pi^2\,\delta(k_x + k_{xp})\,\delta(k_y + k_{yq}) \tag{13}$$

$$\tilde{\boldsymbol{J}}_i(k_x, k_y) = \boldsymbol{J}_{io}\,4\pi^2\delta(k_x + k_{ix})\,\delta(k_y + k_{iy})$$
$$\tilde{\boldsymbol{M}}_i(k_x, k_y) = \boldsymbol{M}_{io}\,4\pi^2\delta(k_x + k_{ix})\,\delta(k_y + k_{iy}).$$

Using the Green's functions for the sources of the electric and magnetic currents evaluated by the boundary conditions of Eqs.(9a) and (9b), the scattered electric field in each region is given by

$$\begin{aligned}\boldsymbol{E}_1(x, y, z) &= \frac{1}{ab}\sum_p\sum_q \tilde{\tilde{\boldsymbol{K}}}_1(k_{xp}, k_{yq})\cdot\tilde{\boldsymbol{J}}_{co}(k_{xp}, k_{yq})\,e^{-j\boldsymbol{k}_{1xpq}\cdot\boldsymbol{r}} \\ &\quad + \{\tilde{\tilde{\boldsymbol{K}}}_1(k_{xp}, k_{yq})\cdot\boldsymbol{J}_{io} + \tilde{\tilde{\boldsymbol{L}}}_1(k_x, k_y)\cdot\boldsymbol{M}_{io}\}\,e^{-j\boldsymbol{k}_{1i}\cdot\boldsymbol{r}}\end{aligned} \tag{14}$$

$$\begin{aligned}\boldsymbol{E}_2(x, y, z) &= \frac{1}{ab}\sum_p\sum_q \tilde{\tilde{\boldsymbol{K}}}_2(k_{xp}, k_{yq})\cdot\tilde{\boldsymbol{J}}_{co}(k_{xp}, k_{yq})\,e^{-j\boldsymbol{k}_{2xpq}\cdot\boldsymbol{r}} \\ &\quad + \{\tilde{\tilde{\boldsymbol{K}}}_2(k_{xp}, k_{yq})\cdot\boldsymbol{J}_{io} + \tilde{\tilde{\boldsymbol{L}}}_2(k_x, k_y)\cdot\boldsymbol{M}_{io}\}e^{-j\boldsymbol{k}_{2i}\cdot\boldsymbol{r}}\end{aligned} \tag{15}$$

where $\tilde{\tilde{\boldsymbol{K}}}$ and $\tilde{\tilde{\boldsymbol{L}}}$ are the dyadic Green's functions for the sources of the electric and magnetic currents, given by Eqs.(A-3) and (A-4) in the Appendix. In addition, $\boldsymbol{k}_{1(2)i}$ and $\boldsymbol{k}_{1(2)pq}$ are the wave-number vectors for the incident wave and the Floquet mode of (p, q).

Substituting Eq.(14) into Eq.(9c), we use the moment method. Then, the current distribution on the conducting element is determined. The current distribution is expanded in a set of N piecewise sinusoidal (*PWS*) basis functions:

$$\boldsymbol{J}_{co}(x, y) = \sum_{n=1}^{N} I_n\,\boldsymbol{J}_n(x, y) \tag{16}$$

where I_n is the unknown amplitude for the element and $\boldsymbol{J}_n(x, y)$ is the n-th basis function. We substitute Eq.(16) into Eq.(9c). The both sides are multiplied by $\boldsymbol{J}_m^*$ and then integrated over the unit cell area. The result is

$$\sum_{n=1}^{N} Z_{mn}\,I_n = V_m \qquad (m = 1, 2, \cdots, N) \tag{17}$$

$$Z_{mn} = \frac{1}{ab}\sum_p\sum_q \tilde{\boldsymbol{J}}_m^*(k_{xp}, k_{yq})\cdot\{\tilde{\tilde{\boldsymbol{K}}}_1(k_{xp}, k_{yq}) - R\bar{\bar{I}}\}\cdot\tilde{\boldsymbol{J}}_n(k_{xp}, k_{yq})$$

$$V_m = -\{\widetilde{J_m}^*(k_{ix}, k_{iy}) \cdot E_{io} + \widetilde{J_m}^*(k_{ix}, k_{iy}) \cdot \widetilde{\widetilde{K_1}}(k_{ix}, k_{iy}) \cdot J_{io} + \widetilde{J_m}^*(k_{ix}, k_{iy}) \cdot \widetilde{\widetilde{L_1}}(k_{ix}, k_{iy}) \cdot M_{io}\}. \tag{18}$$

The algebraic equation of Eq.(17) is solved for the unknown I_n and the current distribution is determined. Then the scattered field can be calculated by Eqs.(14) and (15).

2.3 Features of *FSS*

The z component of the complex Poynting vector expresses the power which flows normal to the interface ($z=0$). By applying the boundary conditions Eqs. (9a), (9b) and (9c) to this Poynting vector, we obtain

$$(1/2)(E_1 \times H_1^*) \cdot a_z + (1/2)(E_i \times H_i^*) \cdot a_z = -(1/2)(E_2 \times H_2^*) \cdot (-a_z) - (1/2) RJ_c \cdot J_c^*. \tag{19}$$

Both sides of the above equation are integrated over the unit cell area and then the conservation law of energy is obtained

$$P_r - P_{in} = -P_t - P_l$$

with

$$\begin{aligned} P_{in} &= (1/2) \iint_{uc} E_i \times H_i \cdot (-a_z)\, ds \\ P_r &= (1/2) \iint_{uc} E_1 \times H_1 \cdot a_z ds \\ P_t &= (1/2) \iint_{uc} E_2 \times H_2 \cdot (-a_z)\, ds \\ P_l &= (1/2) \iint_{uc} RJ_c \cdot J_c^*\, ds \end{aligned} \tag{20}$$

where P_{in}, P_r and P_t are the power of the incident, reflected and transmitted waves, respectively and P_l is the power of the conducting loss. So, the power reflection and transmission coefficients are given by

$$\begin{aligned} R_p &= P_r / P_{in} \\ T_p &= P_t / P_{in}. \end{aligned} \tag{21}$$

3. Numerical results and discussion

In this paper, we treat the reflected and transmitted fields as radiation from the sources of the equivalent electric and magnetic currents. Then, we express the fields by the Green's functions. This scattering problem can be treated separately in the absence of the conducting elements and in the absence of the dielectric

substrate and can be evaluated independently.

We confirm the validity of this theory. First of all, in the absence of the conducting elements, the scattering from a dielectric substrate in free space is presented. Then, the calculated values of reflection coefficient against thickness of the dielectric substrate are compared with the numerical results by *Hounoki, et.al*[2] and the results are shown in Figs.2(a) and 2(b). Since these results are in good agreement, we find that the idea of the equivalent electric and magnetic currents is valid. So, the Green's function for each current describes the effect of the dielectric substrate exactly.

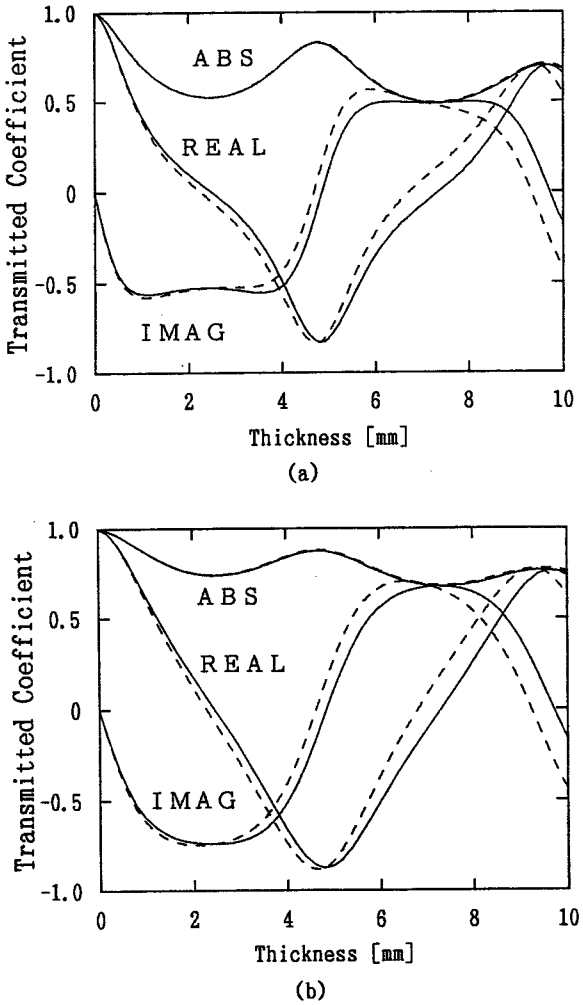

Fig. 2 Comparison of transmitted coefficients of dielectric substrates ;
(a) *TE* incidence (b) *TM* incidence ;
f=11.85 [GHz] , θ =40 [degrees] , ε_r=7.2, $\tan\delta$ =0.065 ;
(– – –) Calculated by *Hounoki, et. al*[2] ;
(——) Calculated for this paper.

Secondly, in the absence of the dielectric substrate, *i.e.*, an infinite periodic array of rectangular patches (a = b = 20.0mm, $l_1 = l_2 = 10.0$mm) in free space is considered. In the following calculation, we analyze scattering by *TM* incidence. Comparing the calculated values of the power reflection coefficient as a function of frequency with the numerical results by *Jin* and *Volakis*[3] in Fig.3, reasonable agreement is obtained over the wide frequency range. Therefore, we make sure

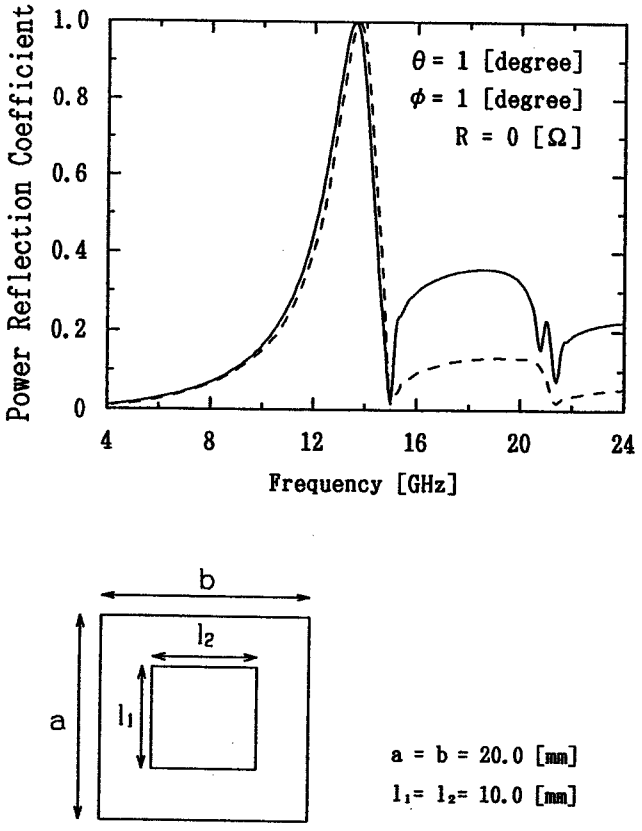

Fig. 3 Comparison of power reflection coefficients of patch elements in free space ;
(– – –) Calculated by *Jin* and *Volakis*[3] ;
(———) Calculated for this paper.

that the behavior of space harmonics for the electromagnetic field and *PWS* expansion modes for the current distribution on the conducting elements are right.

In order to examine about the scattering which the combination of a dielectric substrate and resistive elements affect, we calculate for an infinite periodic array of rectangular patches on a semi-infinite dielectric substrate in Figs. 4, 5 and 6. Figure 4 shows characteristics against frequency for values of the surface resistance. Comparing the resonant frequency where power reflection coefficient

approaches unity with that of Fig.3, we find that the wave-length reduction appears. In addition, the power reflection coefficient is diminished as the surface resistance is increased. The greatest difference in the power reflection coefficient of resistive elements, as compared with that of a perfect conducting elements occurs when the frequency of the incident field is near resonant. Since the conducting loss is proportional to square of the current, we find out that the loss increases around in the resonant frequency where the magnitude of the induced current is large and the power reflection coefficient is diminished.

Figure 5 shows the reflection characteristics against incident angle for values of the surface resistance at the resonant frequency 7.9 GHz. We solve an angle of the Floquet mode which the z component of the propagation constant becomes imaginary and calculate that a grating lobe characteristic of the periodic structure emerges at $\theta = 64^{\circ}$. The Floquet mode comes not to carry power below the angle. The power reflection coefficient is turned out to be diminished as the surface resistance is increased.

In Fig.6, the relative powers of the transmitted, reflected and lost waves are plotted against surface resistance at the resonant frequency 7.9 GHz. The lost power peaks at 30 Ω, with the power reflection coefficient approaching 0.1 at high surface resistance. This power reflection coefficient 0.1 is caused by the scattering from the dielectric substrate.

Finally, we calculate for an infinite periodic array of circular loops (a = b = 20.0mm, r = 8.0mm, w = 1.27mm) on a semi-infinite dielectric substrate and show in Fig.7. Comparing with the characteristics of rectangular patches in Fig.4, we find that of circular loops to be of wider frequency band.

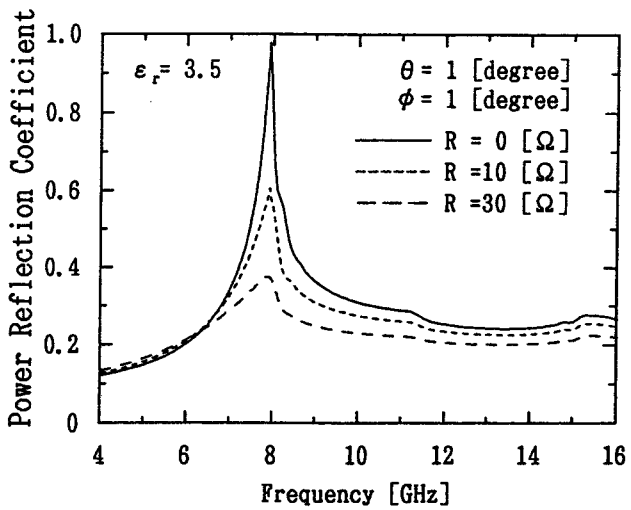

Fig. 4 Power reflection coefficients versus frequency of patch elements.

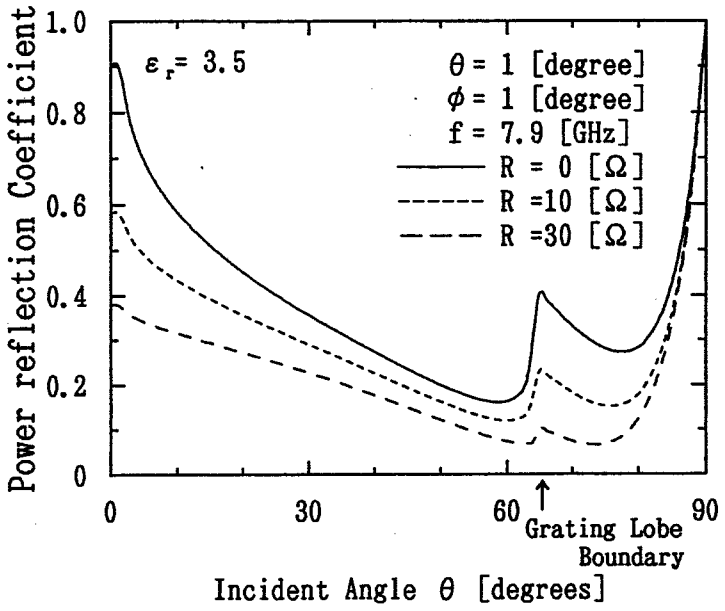

Fig. 5 Power reflection coefficients versus incident angle of patch elements.

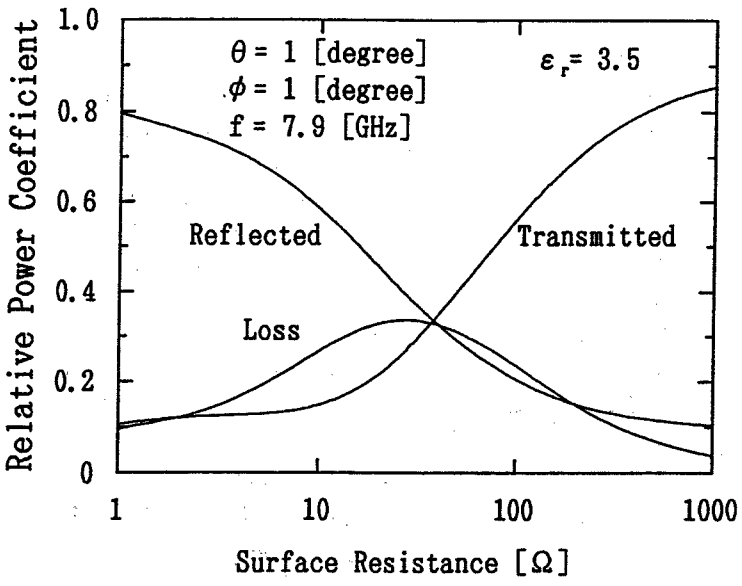

Fig. 6 Relative power coefficients versus surface resistance of patch elements.

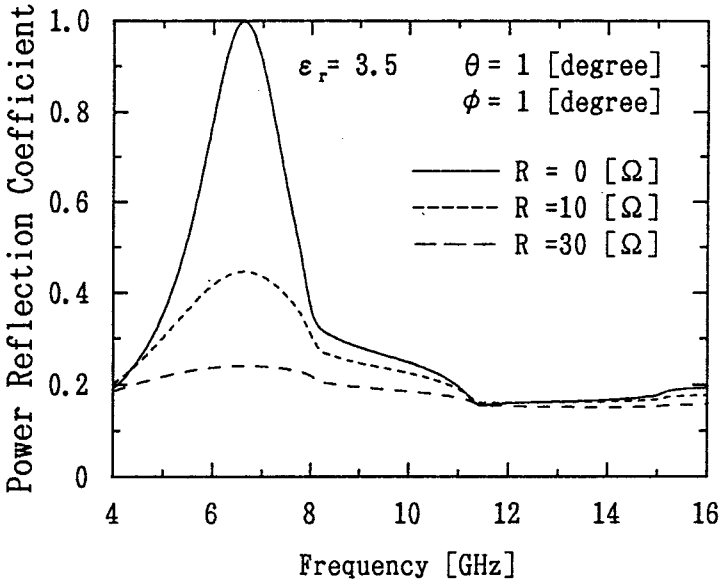

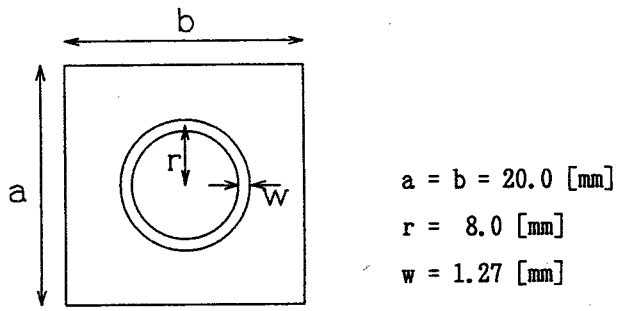

Fig. 7 Power reflection coefficients versus frequency of loop elements.

4. Conclusion

Scattering from a periodic array of arbitrarily shaped conducting elements on a semi-infinite substrate has been analyzed. The solution is based on the moment method in the spectral domain.

In order to treat the scattered field from the conductor and from the surface of the dielectric substrate in a unified method, we introduced the equivalent electric and magnetic currents and then expressed the scattered field by the

Green's function for each current as usual. We examined the characteristics by calculation and compared the results with that of other papers. We made sure that the Green's functions is adequate and confirmed the validity of this theory. In addition, we considered the *FSS* over the dielectric lens and have analyzed the scattering problem by an infinite periodic array on semi-infinite dielectric substrate. Also we discussed out the effect of the surface resistance.

Since this theory is flexible when applied to other various shapes, we will analyze the scattering problem by a periodic array of more complicated elements such as the circularly-polarized devices.

Appendix

The Green's functions and the electromagnetic fields

By using the immittance approach[4], $(\boldsymbol{E}_1, \boldsymbol{H}_1)$ and $(\boldsymbol{E}_2, \boldsymbol{H}_2)$ can be written as

$$\begin{aligned}\boldsymbol{E}_1(x, y, z) &= \frac{1}{4\pi^2}\iint_{-\infty}^{\infty}\{\widetilde{\widetilde{K}}_1(k_x, k_y)\cdot\widetilde{\widetilde{J}}(k_x, k_y) \\ &\quad +\widetilde{\widetilde{L}}_1(k_x, k_y)\cdot\widetilde{\widetilde{M}}(k_x, k_y)\}\, e^{-j(k_x x+k_y y-\gamma z)}\, dk_x dk_y \qquad \text{(A-1)}\end{aligned}$$

$$\begin{aligned}\boldsymbol{E}_2(x, y, z) &= \frac{1}{4\pi^2}\iint_{-\infty}^{\infty}\{\widetilde{\widetilde{K}}_2(k_x, k_y)\cdot\widetilde{J}(k_x, k_y) \\ &\quad +\widetilde{\widetilde{L}}_2(k_x, k_y)\cdot\widetilde{\widetilde{M}}(k_x, k_y)\}\, e^{-j(k_x x+k_y y-\gamma z)}\, dk_x dk_y \qquad \text{(A-2)}\end{aligned}$$

where $\widetilde{\widetilde{K}}_1$ and $\widetilde{\widetilde{K}}_2$ are the dyadic Green's functions for the electric current. $\widetilde{\widetilde{L}}_1$ and $\widetilde{\widetilde{L}}_2$ are the dyadic Green's functions for the magnetic current. These dyadic Green's functions are given by

$$\left.\begin{aligned}
\widetilde{K}_{1xx} &= \widetilde{K}_{2xx} = \frac{1}{\omega\varepsilon_0}\left(\frac{k_x^2}{T_m} - \frac{k_0^2}{T_e}\right) \\
\widetilde{K}_{1xy} &= \widetilde{K}_{1yx} = \widetilde{K}_{2xy} = \widetilde{K}_{2yx} = \frac{1}{\omega\varepsilon_0}\frac{k_x k_y}{T_m} \\
\widetilde{K}_{1yy} &= \widetilde{K}_{2yy} = \frac{1}{\omega\varepsilon_0}\left(\frac{k_y^2}{T_m} - \frac{k_0^2}{T_e}\right) \\
\widetilde{K}_{1xz} &= -\frac{1}{\gamma_1}(k_x\widetilde{K}_{1xx} + k_y\widetilde{K}_{1yx}) \\
\widetilde{K}_{1zy} &= -\frac{1}{\gamma_1}(k_x\widetilde{K}_{1xy} + k_y\widetilde{K}_{1yy}) \\
\widetilde{K}_{2xz} &= \frac{1}{\gamma_2}(k_x\widetilde{K}_{2xx} + k_y\widetilde{K}_{2yx})
\end{aligned}\right\} \qquad \text{(A-3)}$$

$$
\left.
\begin{aligned}
\tilde{K}_{2xy} &= \frac{1}{\gamma_2}(k_x\tilde{K}_{2xy} + k_y\tilde{K}_{2yy}) \,, \\
\tilde{L}_{1xx} &= \tilde{L}_{2xx} = \frac{(1-\varepsilon_r)\,k_x\,k_y}{T_m\,T_e} \\
\tilde{L}_{1xy} &= -\{\frac{\gamma_2}{T_e} + \frac{(1-\varepsilon_r)\,k_x^2}{T_m\,T_e}\} \\
\tilde{L}_{1yx} &= \frac{\gamma_2}{T_e} + \frac{(1-\varepsilon_r)\,k_y^2}{T_m\,T_e} \\
\tilde{L}_{1yy} &= \tilde{L}_{2yy} = \frac{(\varepsilon_r-1)\,k_x\,k_y}{T_m\,T_e} \\
\tilde{L}_{2xy} &= \frac{\gamma_2}{T_m} + \frac{(1-\varepsilon_r)\,k_y^2}{T_m\,T_e} \\
\tilde{L}_{2yx} &= -\{\frac{\gamma_2}{T_m} + \frac{(1-\varepsilon_r)\,k_y^2}{T_m\,T_e}\} \\
\tilde{L}_{1xx} &= -\frac{1}{\gamma_1}(k_x\tilde{L}_{1xx} + k_y\tilde{L}_{1yx}) \\
\tilde{L}_{1xy} &= -\frac{1}{\gamma_1}(k_x\tilde{L}_{1xy} + k_y\tilde{L}_{1yy}) \\
\tilde{L}_{2xx} &= \frac{1}{\gamma_2}(k_x\tilde{L}_{2xx} + k_y\tilde{L}_{2yx}) \\
\tilde{L}_{2xy} &= \frac{1}{\gamma_2}(k_x\tilde{L}_{2xy} + k_y\tilde{L}_{2yy})
\end{aligned}
\right\} \qquad \text{(A-4)}
$$

with

$$
\begin{aligned}
T_m &= \varepsilon_r\gamma_1 + \gamma_2 \\
T_e &= \gamma_1 + \gamma_2 .
\end{aligned} \qquad \text{(A-5)}
$$

References

1) Y.Irimajiri, T.Takano and M.Tokumaru, IEICE, B-Ⅱ, Vol.J73-B-Ⅱ,1,p.20 (1990)
2) K.Hounoki, M.Mikkaichi and A.Takahashi, A•P88-31,p.43 (1988).
3) J.M.Jin and J.L.Volakis, IEEE Trans. Vol.38,4,p.556 (1990).
4) T.Itoh and W.Menzel, IEEE Trans. AP-29,1,p.63 (1981).
5) T.A.Cwik and R.Mittra, IEEE Trans. AP-35,11,p.1226 (1987).